Hindawi Publishing Corporation
Mathematical Problems in Engineering
Volume 2014, Article ID 957041, 12 pages
http://dx.doi.org/10.1155/2014/957041

Research Article

Position Control of Pneumatic Actuator Using Self-Regulation Nonlinear PID

Syed Najib Syed Salim,[1] Mohd Fua'ad Rahmat,[2] Ahmad 'Athif Mohd Faudzi,[2,3] Zool H. Ismail,[2,3] and Noorhazirah Sunar[2]

[1] *Department of Control, Instrumentation and Automation, Faculty of Electrical Engineering, Universiti Teknikal Malaysia Melaka, Hang Tuah Jaya, 76100 Durian Tunggal, Melaka, Malaysia*
[2] *Department of Control and Mechatronics Engineering, Faculty of Electrical Engineering, Universiti Teknologi Malaysia, 81310 Skudai, Malaysia*
[3] *Center for Artificial Intelligence and Robotics, Universiti Teknologi Malaysia, 54100 Kuala Lumpur, Malaysia*

Correspondence should be addressed to Mohd Fua'ad Rahmat; fuaad@fke.utm.my

Received 26 February 2014; Accepted 28 May 2014; Published 22 June 2014

Academic Editor: Jun-Juh Yan

The enhancement of nonlinear PID (N-PID) controller for a pneumatic positioning system is proposed to improve the performance of this controller. This is executed by utilizing the characteristic of rate variation of the nonlinear gain that is readily available in N-PID controller. The proposed equation, namely, self-regulation nonlinear function (SNF), is used to reprocess the error signal with the purpose of generating the value of the rate variation, continuously. With the addition of this function, a new self-regulation nonlinear PID (SN-PID) controller is proposed. The proposed controller is then implemented to a variably loaded pneumatic actuator. Simulation and experimental tests are conducted with different inputs, namely, step, multistep, and random waveforms, to evaluate the performance of the proposed technique. The results obtained have been proven as a novel initiative at examining and identifying the characteristic based on a new proposal controller resulting from N-PID controller. The transient response is improved by a factor of 2.2 times greater than previous N-PID technique. Moreover, the performance of pneumatic positioning system is remarkably good under various loads.

1. Introduction

Pneumatic actuators are widely used in various industrial applications, particularly for those involving manufacturing systems, such as pick and place motion, robot manipulator, and rivet machine. It is reliable, fast acting with high accelerations, of low cost, flexible in installation, simple to maintain, of high power to weight ratio, and free from overheating in the case of constant load [1, 2]. It is an alternative to hydraulic actuators when cleanliness is one of the requirements. However, this actuator exhibits highly nonlinear characteristic due to high friction forces, compressibility of air, and dead band of the spool movement in the valve. These nonlinearities make an accurate position control of a pneumatic actuator difficult to achieve. Research on these groups of actuators has increased in 1990s due to many control strategies that had been tested to the system such as PID control, PD plus, sliding mode control, robust control, adaptive control, and PWM control [3–6]. Meanwhile, more advanced control strategies are aggressively investigated and applied on the early 2000s onward such as the research reported by [7–11]. Consequently, in the last 10 years, the performance of pneumatic positioning system is continuously improved.

The dynamic model of the pneumatic actuator is characterized by significant nonlinearities. Therefore, it is difficult for linear controllers such as PID to provide satisfactory performance for such a system, especially when there is a change in load. However, it can be rectified by modifying its structure to increase the flexibility of the control parameters. In [12], an automatic tuning method to control the position accurately has been proposed. The control algorithm used is an enhanced PID control that augmented with velocity and

acceleration feed forward, bounded integral action, and nonlinear friction compensation. Experimental results for step response indicate that the steady state error was 0.2 mm with overshoot. Previously, the modification of PID controller has been performed by adding the bounded integral action, position feed forward, and friction compensation as reported in [13]. The impact of this modification has improved the performance of the controller. The robustness has increased sixfold in the system mass and was able to follow the S curve trajectory smoothly without affecting the performance in steady state condition. Moreover, the results indicate that the use of friction compensation was able to reduce the steady state error by 40%.

In a subsequent study, a practical control strategy based on modification of PID controller by adding acceleration feedback and nonlinear compensation has been proposed by [5]. Position compensation algorithm with time delay minimization was realized to achieve the position target precisely. The result with different levels of offset showed an improvement compared to conventional PID controller. Besides, the stability of the system has much improved by using acceleration feedback. The implementation of fractional-order controller for pneumatic position servosystem has been investigated by [14]. In this research, the FOPID controllers $PI^{\lambda}D^{\delta}$ are implemented. The aim of their study is to solve the strong nonlinearity and low natural frequency problem. In the other research, authors in [15] have proposed a combination of the conventional PID controller with fuzzy logic inference in which the parameters of the conventional controller were tuned automatically to obtain the precise position control of pneumatic actuator. Moreover, a friction compensation and stabilization algorithm was added to ensure that the accurate positioning be achieved. The results indicate that the positioning accuracy was within the margin of 1 mm. The study on combination between PID and fuzzy logic is also reported in [16]. In this study, stability of the controller is theoretically proved according to the small gain theorem. Experimental results signify that the proposed fuzzy PID has better performance than classical PID.

With the reason of PID control being vastly popular control strategy in the industry, a mixture of conventional PID controller and the neural network, which has powerful capability of learning, adaptation, and tackling nonlinearity, has been proposed by [10]. The experiments have been carried out in practical pneumatic artificial muscle for both cases without and with external inertia load up to 20 kg cm^2. Comparison with conventional PID controller has shown that the proposed method presents better performance and has the ability to compensate the disturbance. In another research suggested by [11], an adaptive fuzzy PD controller is used to compensate the friction. The aim is to ensure the movement of the stroke to the set point quickly and precisely without significant overshoot. The authors claimed that the settling time and steady state error under constant load have obtained less than 1 s and 0.3 mm, respectively, without significant overshoot. In the other research, due to the drawback of adaptive controllers that are not fast enough to follow the parameter variation, a multimodel controller based on several fixed PD-controllers is recommended by [17]. This technique was proposed for the position control of a pneumatic cylinder under variable loads. Five PD controllers had been tuned based on the estimated model for the five fixed loads that has been identified earlier. Experimental results show that this technique successfully improved the ability in producing outstanding performances even under variable load conditions.

In previous work, PID controller that incorporates with nonlinear gain, namely, N-PID controller, was designed to control the position and tracking of pneumatic actuator [18]. The nonlinear gain is used to reduce overshoot when the relatively large gain is utilized. Experimental results indicate that the performance of the system with N-PID controller has significantly improved referring to its capability to perform with load up to 20 kg. In this paper, the enhancement of the nonlinear PID controller is proposed to improve the performance especially in the transient part. Recap that the N-PID controller has two parameters, namely, range of variation ($e_{\max}$) and rate of variation (α) [18–20]. Those parameters need to be determined in advance. It is intricate to choose the appropriate combination of these parameters. To overcome this difficulty, modifications have been made with the purpose of generating these parameters automatically which is dependent on the changes of error. This indirectly contributes to the time reduction in determining the parameters and makes it more flexible with respect to the changes in position.

This paper is organized as follows. In Section 2, mathematical modelling of the pneumatic actuator is described. In Section 3, a self-regulation nonlinear PID (SN-PID) controller is described in detail. In Section 4, the proposed method is simulated using MATLAB/SIMULINK. Subsequently, experiments are carried out to verify the effectiveness of the proposed method in real time and analysis of performance under variation of load has been investigated. Finally, Section 5 contains some concluding remarks.

2. System Model

The system consists of

(i) 5/3 bidirectional proportional control valve (Enfield LS-V15s),

(ii) double acting with double rod cylinder,

(iii) noncontact micropulse displacement transducer with floating magnet (Balluff BTL6),

(iv) data acquisition card (NI-PCI-6221 card),

(v) pressure sensors (WIKA S-11),

(vi) personal computer and,

(vii) Jun Air Compressor.

The pneumatic cylinder with 500 mm stroke for both sides and 40 mm in diameter is fixed on the base. One side of the piston rod is connected to the carriage and drives an inertial load on guiding rails. The displacement transducer is fixed

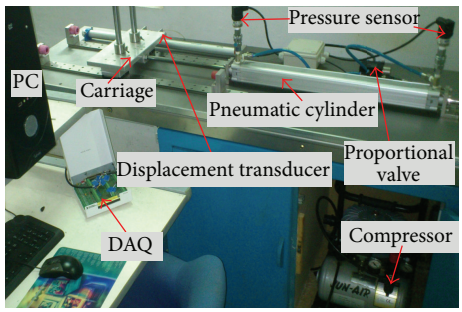

Figure 1: Pneumatic positioning system experimental setup.

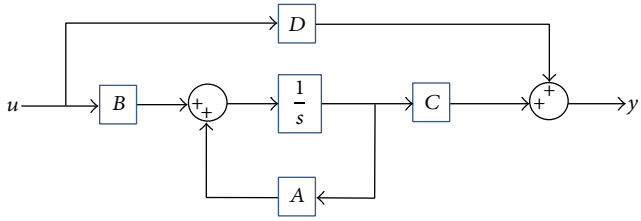

Figure 2: State-space model structure.

in parallel with the rail where the carriage is mounted. The data acquisition and control routines that were implemented under real-time workshop in MATLAB are realized by PC equipped with a PCM card. Two pressure sensors are installed on both sides of the cylinder that allows the measurement of differential pressure between two chambers. Figure 1 shows the experimental setup used to validate the proposed method.

2.1. Mathematical Modelling. Since the design is based on modification PID controller, system identification is employed to obtain the transfer function of the system. The experiments were conducted starting with collecting the input and output data based on open loop system with sampling time of 0.01 second. The input signal with multiamplitude and frequency sine wave is used where 2000 numbers of data have been collected. A state space model as shown in Figure 2 is used as a model structure of the system. Synthesis of the state space control is based upon the following system of equations:

$$\begin{aligned} x(t+Ts) &= Ax(t) + Bu(t) + Ke(t), \\ y(t) &= Cx(t) + Du(t) + e(t), \end{aligned} \tag{1}$$

where $A \in R^{n\times n}$, $B \in R^{n\times m}$, $C \in R^{1\times n}$, and $D \in R^{1\times m}$ represent the matrices of the system, while $x(t) \in R^n$, $y(t) \in R$, $u(t) \in R^m$, and $K \in R^{n\times m}$ represent the state-vector, measured output, measured input signal and noise, respectively. $e(t)$ is the vector that represents the difference between the measured output and the predicted output of the model.

The estimation of the parameters is computed by iterative search for a model through prediction-error minimization (PEM) method that gives the minimal prediction error variance when applied to the working data. Through this method, the parameters of the model are calculated by minimizing a cost function of the prediction errors, giving

$$V_N\left(\theta, Z^N\right) = \frac{1}{N}\sum_{k=1}^{N} e^2(k,\theta), \tag{2}$$

where N denotes the number of data samples. For linear systems the error can be expressed as

$$e(k) = H^{-1}(\theta)\left[y(k) - G(\theta)u(k)\right]. \tag{3}$$

Therefore the parameter estimation can be obtained through (2) and (3) by minimizing V_N as follows:

$$\hat{\theta}_N = \arg\min_{\theta} \frac{1}{N}\sum_{k=1}^{N} H^{-1}(\theta)\left[y(k) - G(\theta)u(k)\right]^2. \tag{4}$$

The following equation is the discrete state-space equation obtained through this identification process:

$$\begin{aligned} A &= \begin{bmatrix} 2.846 & -1.350 & 8.544\times10^{-1} \\ 2 & 0 & 0 \\ 0 & 0.5 & 0 \end{bmatrix}, \qquad B = \begin{bmatrix} 0.125 \\ 0 \\ 0 \end{bmatrix}, \\ C &= \begin{bmatrix} -3.494\times10^{-2} & 3.765\times10^{-2} & -3.967\times10^{-2} \end{bmatrix}, \\ D &= [0]. \end{aligned} \tag{5}$$

The state space in continuous form is then obtained using zero order hold (ZOH) conversion method with sampling time, $Ts = 0.01$ s. This conversion method generates the continuous time input signal by holding each sample value constant over one sample period. The following equation represents continuous state space of the system that has been converted in phase variable form:

$$\begin{aligned} A &= \begin{bmatrix} 0 & 1 & 0 \\ 0 & 0 & 1 \\ -3.887\times10^{-1} & -85.530 & -15.740 \end{bmatrix}, \\ B &= \begin{bmatrix} 0 \\ 0 \\ 1 \end{bmatrix}, \\ C &= \begin{bmatrix} 92.490 & 6.385 & -5.071\times10^{-1} \end{bmatrix}, \\ D &= [0]. \end{aligned} \tag{6}$$

A continuous transfer function then can be defined as

$$Gp(s) = \frac{-0.507s^2 + 6.385s + 92.490}{s^3 + 15.740s^2 + 85.530s + 0.389}. \tag{7}$$

2.2. Dead-Zone of the Valve. Dead-zone is an inevitable phenomenon for the valve which represents a loss of information when the signal falls into the dead-band area. It refers to a situation where at a certain range of input values does not give any output. Dead-zone characteristics are often unknown and can drastically reduce control system performance and lead

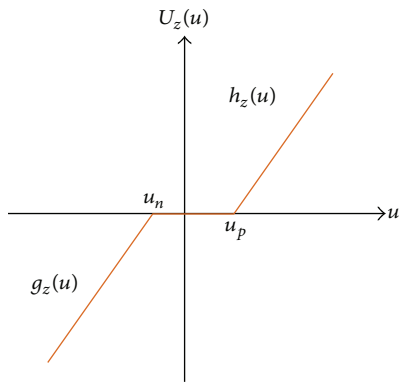

Figure 3: Dead-zone characteristic.

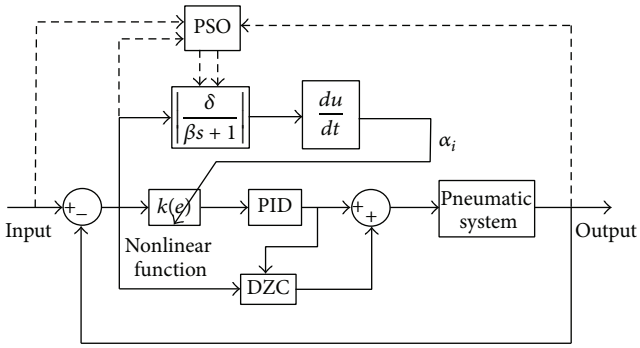

Figure 4: Block diagram of self-regulation nonlinear PID (SN-PID) controller.

to limit cycles in the closed loop system. Figure 3 shows the graphical representation of dead-zone characteristic, $U_z(u)$.

A mathematical model for the dead-zone is given by

$$U_z(u) = \begin{cases} g_z(u) < 0, & u \le u_n, \\ 0, & u_n < u < u_p, \\ h_z(u) > 0, & u \ge u_p, \end{cases} \tag{8}$$

where u_n is negative limit of dead-zone, u_p is positive limit of dead-zone, $g_z(u)$ is negative slope of output, $h_z(u)$ is positive slope of output, U_z is output, and u is input.

3. Control Design

The conventional PID controller emphasizes a straight forward design approach to achieve the favourable result in controlling the position and continuing motion as the ultimate goal. However, as position control performance is more rigorous, this type of controller is often difficult to give the better performance due to the presence of nonlinearities especially in pneumatic systems. In previous work [18], the PID controller that is incorporated with automatic nonlinear gain, namely, nonlinear PID controller, was designed to control the position and tracking of pneumatic actuator. The performance of N-PID controller is better than conventional PID controller in terms of robustness. However, there is still room for improvement especially in the transient part whereby the improvement by imposing a higher force in the initial movement should be implemented to overcome the static friction.

The aim of this paper is to design a controller so that the displacement of this actuator can reach the target quickly and accurately without significant overshoot. For this goal, an additional function was added to the controller in compensating the nonlinearities of the system. This function will continuously generate the value of rate variation (α) to regulate the output of the nonlinear function. The proposed technique is called self-regulation nonlinear PID (SN-PID) controller. This technique is suitable to be used in the industry due to its ability to execute in such a short period of time and effectiveness to reach the performance that is unable to achieve by both conventional PID controller and nonlinear PID controller. The proposed method was indeed more efficient and robust in improving the step response of pneumatic positioning system.

3.1. Design of Self-Regulation Nonlinear PID (SN-PID) Controller. The proposed controller is an enhancement from the N-PID controller. As mentioned in the previous work [18] the N-PID controller is bounded by a sector of nonlinear gain $k_x(e)$. The value of nonlinear gain is continuously changed depending on the changes of error. The appropriate value of both rate variation α and the boundary of maximum error $e_{\max}$ is selected by the user. The value of $e_{\max}$ is set by any value depending on sector where the nonlinear function will take action. In previous work, the parameter of rate variation α is determined based on trial and error after taking into account the stability region of the system. However, the selected value of α is limited to certain circumstances. Besides, the optimal value of α is difficult to determine in producing outstanding performance in terms of speed and chattering avoidance. In this study, the value of α is generated on-line to provide flexibility to the controller. Figure 4 shows the block diagram of the proposed method. The value of nonlinear gain $k_x(e)$ is automatically varied depending on the value of α_i that is on-line generated using proposed equation as defined in

$$\frac{\alpha_i(s)}{e(s)} = \frac{d}{ds}\left|\frac{\delta}{\beta s+1}\right|. \tag{9}$$

This equation is called self-regulation nonlinear function (SNF). It has a simple structure and does not require more computation time. For the purpose to generate α automatically, the relationship between δ and β needs to be determined in advance. The details on how to determine these parameters are described in the next subsection. The nonlinear gain is defined under the limitation of $0 < k_x(e) \le k(e_{\max})$ giving

$$k_x(e) = \frac{\exp(\alpha_i e) + \exp(-\alpha_i e)}{2}, \qquad e = \begin{cases} e & |e| \le e_{\max}, \\ e_{\max}\,\mathrm{sign}(e) & |e| > e_{\max}, \end{cases} \tag{10}$$

where

$$k\left(e_{\max}\right) = -\frac{1}{\left|G\left(j\omega\right)\right|}. \tag{11}$$

The output produced from the nonlinear function is known as a scaled error which is expressed in (12). The whole equation of the proposed SN-PID controller is written as (13).

$$f_x\left(e\right) = k_x\left(e\right) \cdot e\left(t\right), \tag{12}$$

$$u_{\text{PID}} \cdot f_x\left(e\right) = k_p(\cdot)\, e\left(t\right) + k_i\left(\cdot\right) \int_0^t \left[e\left(t\right)\right] dt + k_d\left(\cdot\right) \frac{d}{dt}\left[e\left(t\right)\right], \tag{13}$$

where $(\cdot)$ corresponds to the controller gains that are time varying, which depend on input and other variables.

3.2. Determination of δ and β. In order to identify the relationship between δ and β, a particle swarm optimization (PSO) technique is employed. It is a stochastic optimization technique influenced by simulating the animal social behavior, for example, flocking of birds [21]. This technique is initialized with a group of random solutions (particles) and searches for optima by updating generations. Figure 5 shows the flowchart for PSO algorithm used in this study. Based on this flowchart, each particle randomly reached in the early stages is a candidate solution and has a specific fitness value. These particles will move with a certain velocity which is affected by its own flying experience and other particles flying experience. Through the process, velocity and position are updated with two best values, namely, personal best (*P*best) solution and global best (*G*best) solution. For example, the ith particle is expressed as $x_i = (x_{i,1}, x_{i,2}, \ldots, x_{i,d})$ in d-dimensional space. Previous best position (*P*best) of the ith particle is stored and expressed as $P\text{best}_i = (P\text{best}_{i,1}, P\text{best}_{i,2}, \ldots, P\text{best}_{i,d})$. The best particle index among all the particles in a flock or group is specified as G_{best}. Thus, the velocity and position of each particle can be calculated using the current velocity and distance from *P*best to *G*best as described in (14) and (15), respectively,

$$V_i^{t+1} = w \cdot V_i^t + c_1 \cdot \text{rand}_1\left(\cdot\right) \cdot \left(P\text{best}_i - X_i^t\right) + c_2 \cdot \text{rand}_2\left(\cdot\right) \cdot \left(G\text{best}_i - X_i^t\right), \tag{14}$$

$$X_i^{t+1} = X_i^t + V_i^{t+1}. \tag{15}$$

The value of w is set by (16) as follows:

$$w = w_{\max} - \frac{w_{\max} - w_{\min}}{\text{itr}_{\max}} \times \text{itr}, \tag{16}$$

where w is inertia weight function, c_1 and c_2 are learning factors, rand_1 and rand_2 are random numbers in range $[0, 1]$, $\text{itr}_{\max}$ is maximum number of iterations, and itr is current iteration, $i = 1, 2, 3, 4, \ldots, N_{\text{swarm}}$.

The performance criterion in the time domain as described in (17) is employed for this optimization. It is used in calculating the cost function for evaluating the parameters of self-regulation nonlinear function (SNF). The output response constraint including overshoot, rise time, settling time, and steady state error is taken into account in this performance criterion. The cost function f is a reciprocal of the performance criteria $W(K)$ as defined in

$$W\left(K\right) = \left(M_P + e_{\text{ss}}\right) \cdot \left(1 - e^{-\sigma}\right) + \left(t_S - t_r\right) \cdot e^{-\sigma}, \tag{17}$$

$$f = \frac{1}{W\left(K\right)}, \tag{18}$$

where K is $[\delta, \beta]$ and σ is the weighting factor. According to [22], the value of σ should be larger than 0.7 to reduce steady state error and overshoot. In this study, this value is set equal to 0.9. Referring to (9), as far as stability of the system is concerned, the value of δ should be selected less

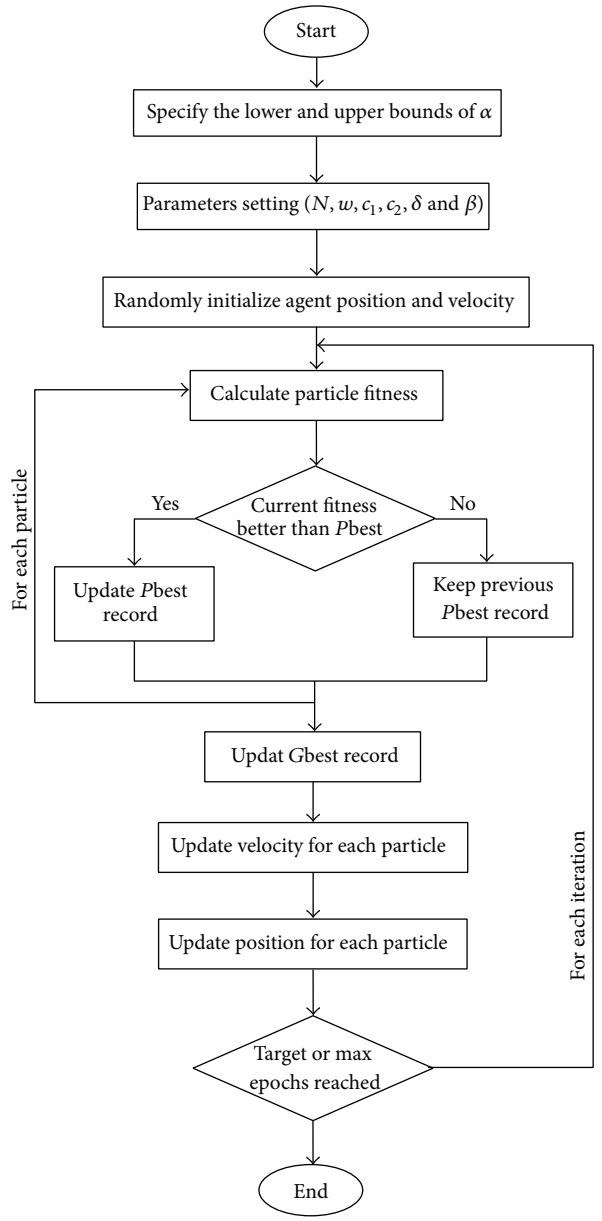

Figure 5: Flow chart for particle swarm optimization technique.

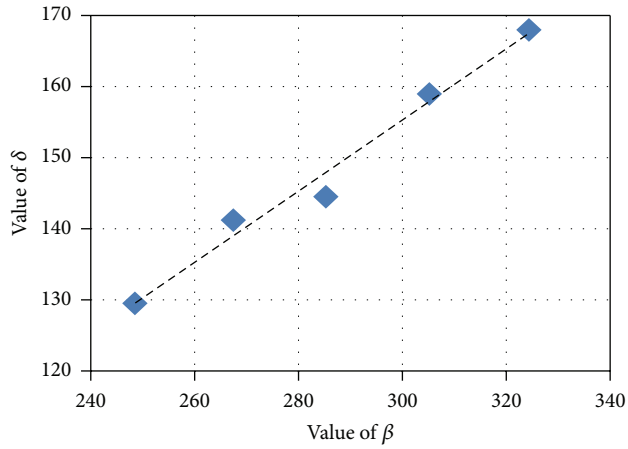

Figure 6: Relationship between δ and β.

than β. Otherwise, the value of rate variation α will extremely increase and it causes the system to become unstable. As mentioned earlier, the value of δ and β can be determined by identifying the relationship between them. For this purpose, the PSO algorithm was run several times and the results of these parameters are tabulated in Table 1. Figure 6 shows the relationship between δ and β based on these optimization processes. From this graph, it can be concluded that δ and β are directly proportional to each other with a slope of 0.51. Through this observation, the equation as expressed in (19) was applied to determine the value of δ and β:

$$\delta = 0.51\beta. \tag{19}$$

Figure 7(a) shows the response produced from SNF for the system tested with step input 200 mm. By differentiating this response, the rate variation α is obtained as presented in Figure 7(b). Based on this response, the rate variation is decreasing starting at 0.13 and ending at 0 where the steady state response is achieved. It indicates that the value of α is high for the beginning of each movement and gradually declines when the piston starts moving. This will drive the system output to its goal rapidly without significant overshoots and be able to prevent excessive oscillations. Moreover, the varying of α will generate the numerous ranges of nonlinear gain, $k_x(e)$, and increase the flexibility of the controller.

3.3. System Stability. In any controller design, it is necessary to ensure the stability of the system. Since the value of rate variation α is generated automatically, the selected value of both weighting factors δ and β should take into account the maximum value of the nonlinear gain $k_x(e)$. The Popov stability criterion is used in determining the maximum value of $k_x(e)$. The absolute stability of the equilibrium states of nonlinear systems by applying Popov criterion is based on the modified amplitude-phase characteristic of the linear part of the system. The procedure to determine the range of $k_x(e)$ using Popov stability criterion has been discussed in detail in [20]. By using Matlab software, the Popov plot of $G(j\omega)$ is crossing the real axis at the point $(-0.14, j0)$ as

Table 1: Parameter determination via particle swarm optimization.

	Op1	Op2	Op3	Op4	Op5
W	0.048	0.030	0.039	0.052	0.041
δ	167.9	141.2	158.9	144.5	129.51
β	324.4	267.5	305.2	285.3	248.53
$\delta : \beta$	0.518	0.528	0.521	0.506	0.521

shown in Figure 8. Based on this information, the maximum value of the nonlinear gain $k(e_{\max})$ can be obtained through (19). Therefore, according to the Popov stability criterion, the range of the allowable nonlinear gain $k_x(e)$ is (0, 7.14).

3.4. Effectiveness of the Proposed Method in Industrial Application. The prerequisite in designing a controller is practicality. Therefore, its ability to be implemented on the real plant is one of the criteria that need to be taken into account. The resulting output of the controller during transient period should be within the limitation of the system hardware. Without taking this into account, the presence of integrator windup phenomenon surely will degrade the performance of the system. This phenomenon occurs when the controller output saturates due to integral terms and this generally leads to large settling times and overshoots. In this study the saturation limit of the hardware is within ±10 volt. Through the proposed method, the controller variables are only allowed to be at saturation point for a short period of time. This can be seen as shown in Figure 9(a) when the multistep command inputs are applied to the system. Where the amplitude of the controller output is only at saturation point in a short period of time which is about 5 ms, even the distance of the movement is increased. The other controllers, namely, SMC and PID, have been applied to the system for comparison purposes. Figure 9(b) illustrates the controller output of this controller when operating under distance of 460 mm. For the purposes of comparison, the output controller for PID and SMC is depicted in Figure 10.

3.5. Design of Dead-Zone Compensator. Due to the existence of dead-zone for the spool movement in opening and closing of the valve, the presence of delay is unavoidable. The dead-zone compensator used in this study is based on the research conducted by [23]. It was implemented by using the following conditions.

(1) If absolute error is small or equal to the desired value of error, the output of DZC is represented by U_{e0};

(2) if absolute error is greater than the desired value of error and the controller output is greater than zero, the output of DZC is represented by u_p;

(3) if absolute error is greater than the desired value of error and the controller output is less than zero, the output of DZC is represented by u_n,

where u_{e0}, u_p, and u_n are input compensation based on error, positive dead-zone compensation, and negative dead-zone compensation, respectively. Based on these conditions, there is no force imposed to the payload when the output of the

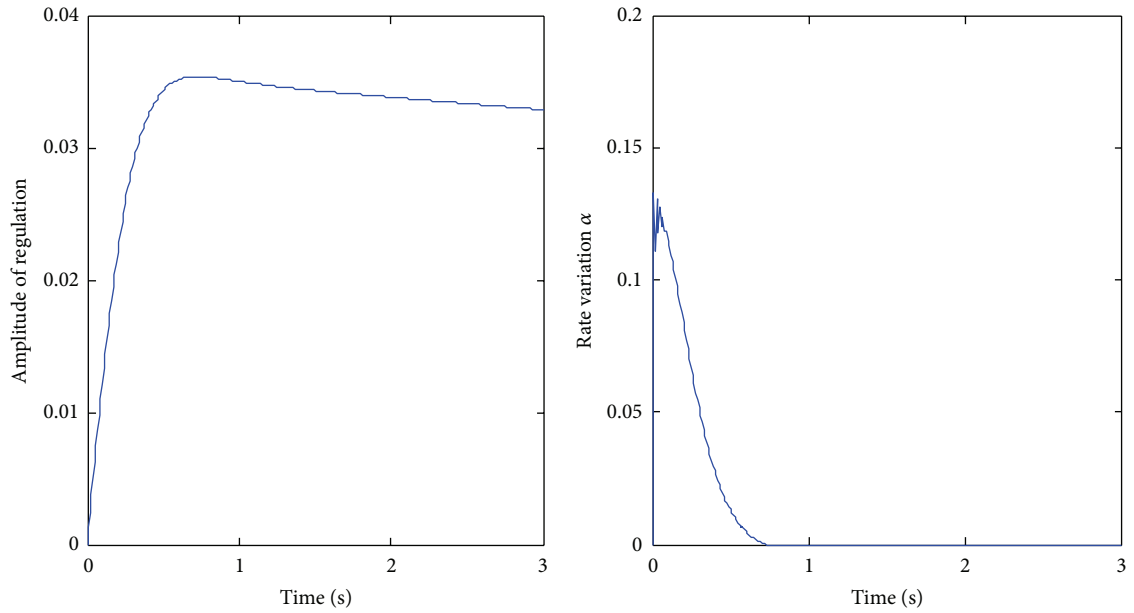

Figure 7: Response of the regulation block diagram: (a) output before differentiating; (b) rate variation.

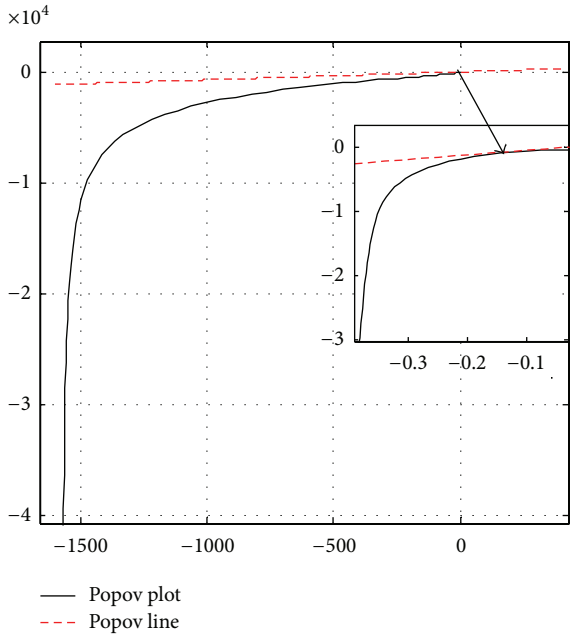

Figure 8: Graphical solution using Popov analysis.

DZC is represented by u_{e0}. For the other conditions in which the position error exceeded e_d in either positive or negative direction, the output of the controller will be added to the dead zone compensators u_p and u_n, respectively.

4. Results and Discussion

Simulation and experimental validation are performed to evaluate the performance of the proposed SN-PID with different step of inputs and various masses of the load. The controller was designed for the system with a nominal payload mass of 3.2 kg. The difference between the nominal and other masses of payload was tested to illustrate the robustness of the proposed controller. The performance of the proposed technique is compared to the other techniques, namely, conventional PID, N-PID, and SMC controller. The parameters of the proposed controller including self-regulation nonlinear function (SNF) and other parameters are tabulated in Table 2. The parameters of the PID should be determined earliest before the other parameters can be obtained. The procedures to obtain PID controller parameters have been given in the previous work [18].

4.1. Simulation Results. In this section, the performances of the proposed method are presented via simulation before being realized in real time. The system which has been simulated with the input consists of a variety of distances. The result indicates that the system has successfully maintained the performance of the system. It can be seen in Figure 11(a) where the transient response is quite similar for each transition of the step input. The changes occur in the value of α for each transition as shown in Figure 11(b)which gives information to the nonlinear function in determining the

Table 2: Parameters of the controller.

Control strategies	Control parameters		
	Name of parameter	Abbreviation	Value
PID	Proportional gain	K_p	2.099
	Integral gain	K_i	9.56×10^{-3}
	Derivative gain	K_d	0.035
	Filter	N	12.207
SN-function	Param 1	δ	129.51
	Param 2	β	248.53
	Variation of error	$e_{\max}$	2
Dead-zone compensator	Control value in the range of desired e_{ss}	u_{e0}	0.01
	+ve dead-zone compensation	u_p	0.5
	−ve dead-zone compensation	u_n	−0.65
	Desired e_{ss}	e_d	0.005

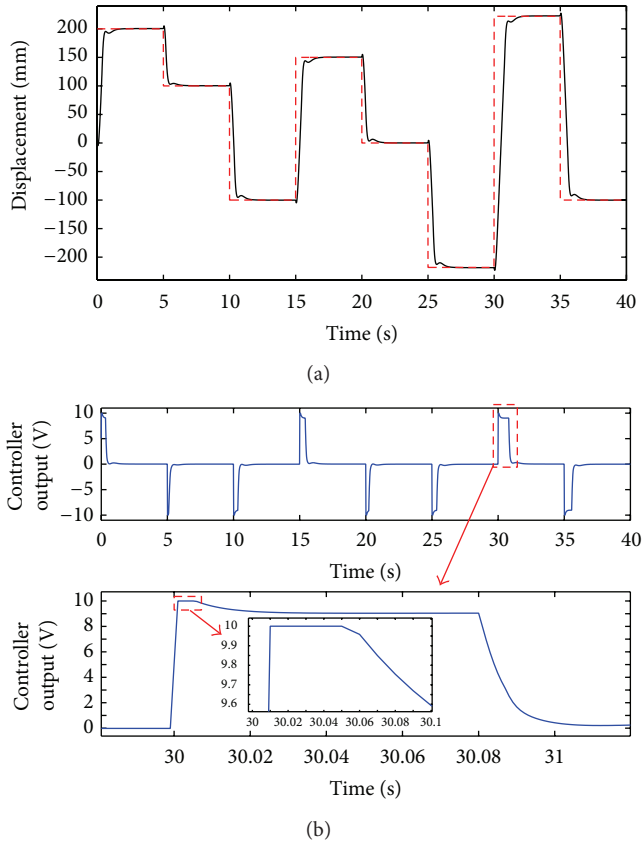

Figure 9: Response for the system with SN-PID: (a) displacement (mm); (b) controller output.

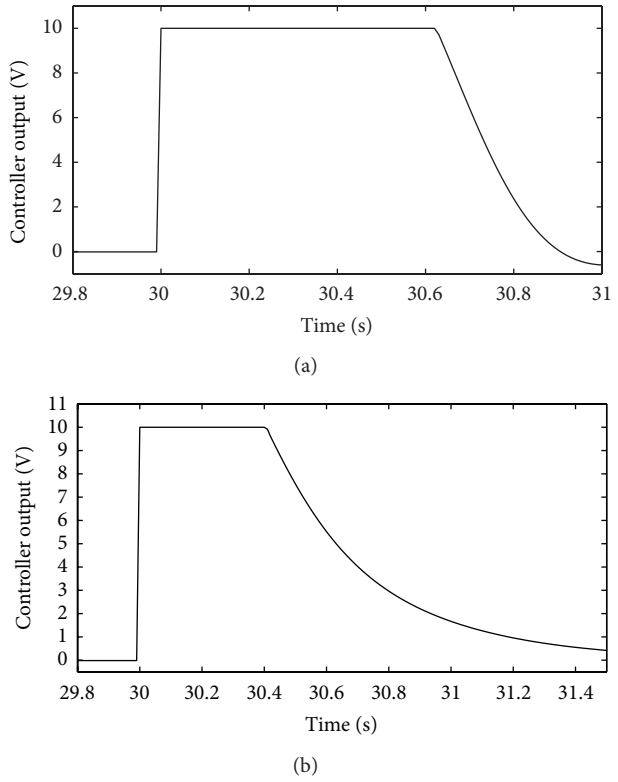

Figure 10: Controller output of the system with (a) PID and (b) SMC.

appropriate value of nonlinear gain, $k_x(e)$. The corresponding response of the controller output is shown in Figure 11(c).

It clearly can be seen that the amplitude of the response is within the limits allowed by the data acquisition card that is used in the experiment which is between −10 v and +10 v. Such a situation is relieving to ensure that the output response may be generated without the overshoot for both simulation and experimental validation. In addition, the signal with random input is also employed to strengthen the evidence that the SN-PID controller can cater various forms of input. This can be observed as indicated in Figure 12(a). The result has confirmed that the proposed controller is able to track the demand even in the case where the input response is changed all of a sudden. Figure 12(b) shows the reaction of the rate

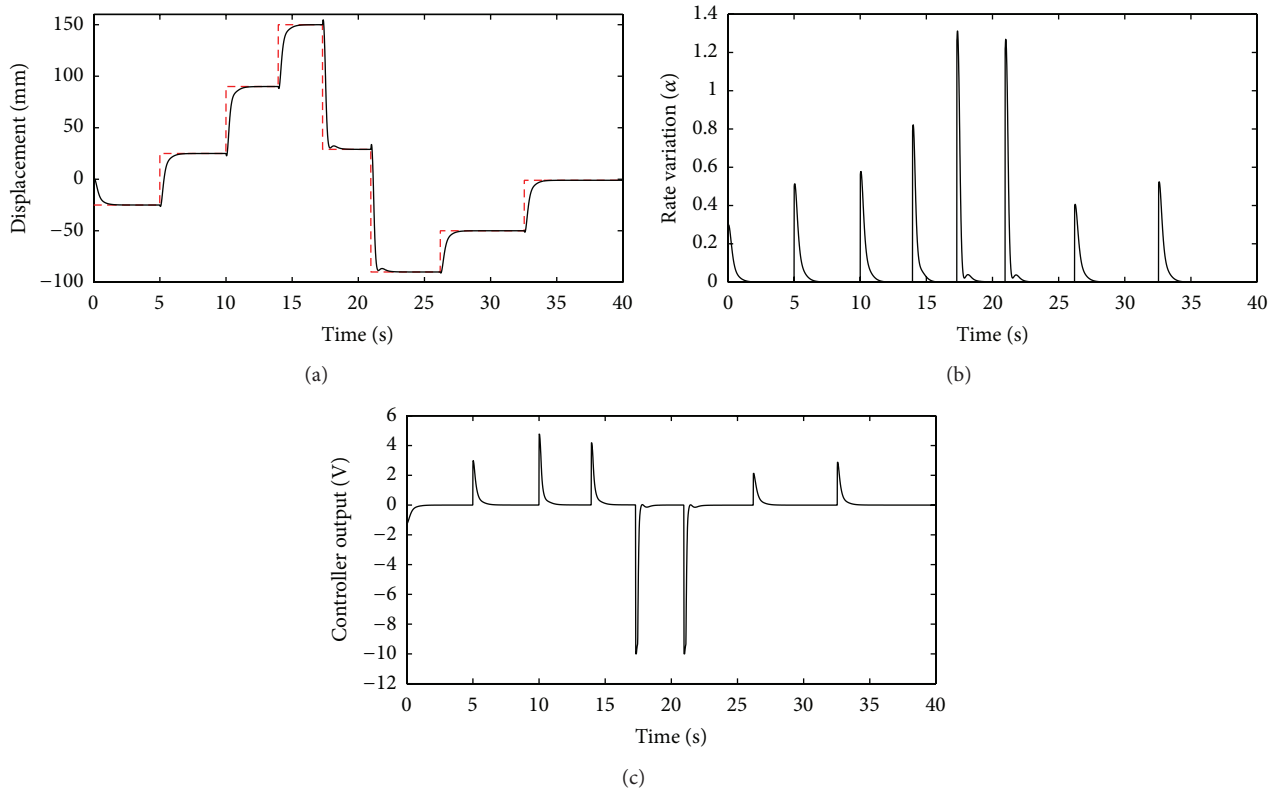

FIGURE 11: Performance of system controller by SN-PID controller: (a) displacement (mm); (b) rate variation α; and (c) controller output (v).

variation (α) which acts as an essential variable in order to ensure that various forms of input can be handled well.

4.2. Experimental Validation. In order to verify the performance of the proposed controller, the result from simulation is compared to the result obtained from the real-time system. As can be seen from Figure 13, the response obtained based on experimental validation is quite similar to the simulation. There is only a slight difference on the transient part in which the response from experimental result is a bit faster compared to the simulation. Subsequently, to strengthen the evidence of the effectiveness of the designed controller, the experiment with various types of input is conducted. These results have confirmed that the acceptable performance is achieved for both experimental validation and simulation where the real-time response of the pneumatic system also looks quite similar to the simulation.

4.3. Performance Analysis on the Variation of Load. One of the issues that need to be taken into account in designing a controller is the ability of the controller to compensate the system when there are changes occurring in the load. In this section, the results from several experiments with different load are combined and investigated. This system is tested using step response with displacement of 400 mm. The moving mass of the horizontal cylinder is attached to the load of 3.2 kg, 8.4 kg, 13.5 kg, 23 kg, and 28 kg. Based on the result as shown in Figure 14 the proposed controller is able to accommodate to the system for various changes of load. Apparently, it can be seen that the proposed technique is able to control the system even when the load is added up to 28 kg. The steady state error under these variations of the load is quite similar which is around 0.01 mm.

4.4. Performance Comparison with the Other Methods. As a benchmark, the proposed controller has been compared to the other methods. The comparison of the performance between the proposed SN-PID, N-PID, conventional PID, and sliding mode control (SMC) is performed using the same test rig. For sliding mode control the sliding surface for third order is defined as follows:

$$S = \ddot{y} - \ddot{y}_d + 2\lambda\left(\dot{y} - \dot{y}_d\right) + \lambda^2\left(y - y_d\right). \quad (20)$$

By taking derivative of (20) and setting $\dot{S} = 0$, the equivalent control signal, u_{eq}, therefore can be obtained by substituting the plant model. The switching control signal as in (21) is

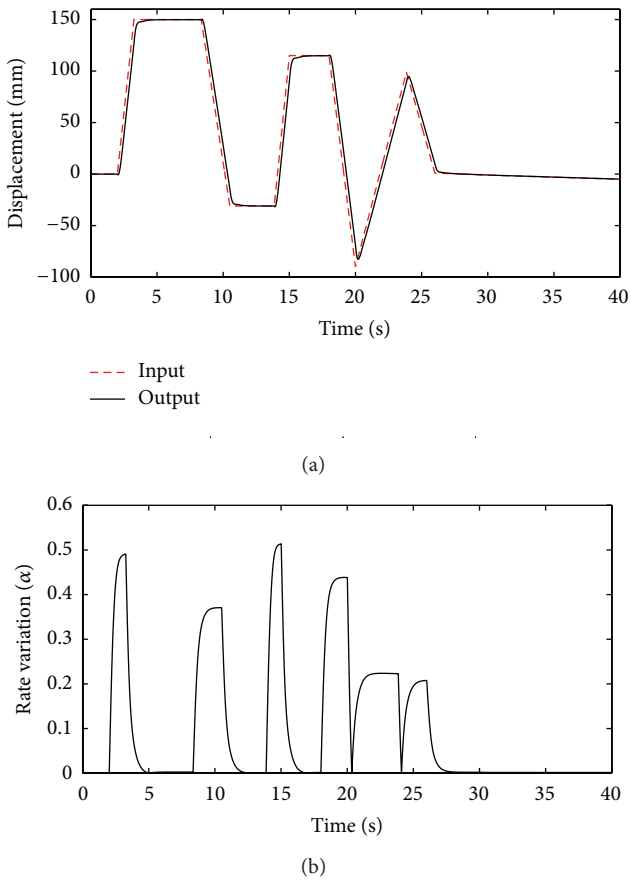

Figure 12: Performance of system controller by SN-PID with various forms of input: (a) output and (b) rate variation α.

employed. The controller parameters are set to the values $\varphi = 1087$ and $\lambda = 36$:

$$u_s = -k_s \operatorname{sat}\left(\frac{S}{\varphi}\right), \tag{21}$$

where

$$\operatorname{sat}\left(\frac{S}{\varphi}\right) = \begin{cases} \dfrac{S}{\varphi}, & \left|\dfrac{S}{\varphi}\right| \leq 1, \\ \operatorname{sign}\left(\dfrac{S}{\varphi}\right), & \left|\dfrac{S}{\varphi}\right| > 1. \end{cases} \tag{22}$$

The results indicate that the proposed controller, namely, SN-PID controller, has performed better compared to the other methods. It can be seen in Figure 15 that the output of the system controlled by SN-PID shows a better performance in transient part compared to others. In the same experiment, the result for the system controlled by N-PID controller is worst in terms of speed compared to others. However, by taking into consideration the robustness of the system, SN-PID and N-PID controller give better performance under various loads compared to the others. This is due to the numbers of oscillation appearing in the output response for the system controlled by conventional PID and SMC as

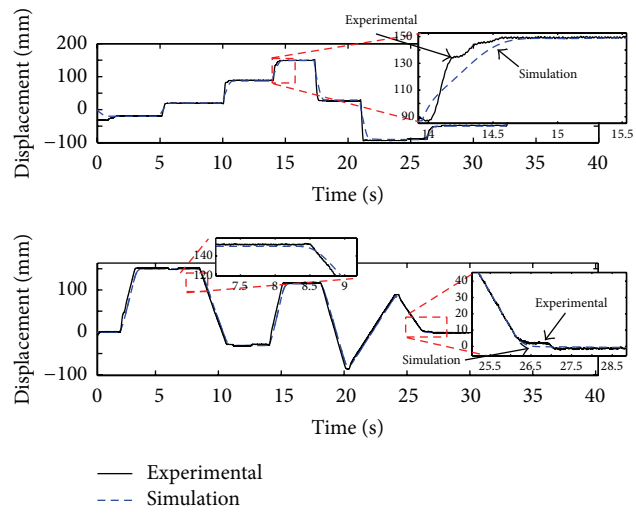

Figure 13: Experimental validations for the system with SN-PID controller.

depicted in zoom-in view. Moreover, based on the results as illustrated in Figure 14 it has been proved that the SN-PID controller is able to operate under variations of load up to 28 kg. The steady state error for the system controlled by SN-PID and N-PID is about 0.01 mm, while for the system controlled by other controllers it is about 0.1 mm to 0.5 mm.

5. Conclusion

In this research, a new technique, namely, self-regulation nonlinear PID (SN-PID) controller, is proposed and designed to control the position of pneumatic actuator system. The purpose of this technique is to enhance the performance of nonlinear PID (N-PID) controller that was tested to the system previously. This was performed by utilizing the characteristic of rate variation of nonlinear gain via equation which is known as regulation function. The purpose of this technique is to make the controller be flexible with several sector-bounded of gain. Simulations and experiments were conducted to verify the performance of the proposed technique and found that the transient response is improved by a factor of 2.2 times better than previous N-PID technique with better steady state response. In addition, the experimental results also confirmed that the SN-PID controller is capable of keeping up the performance under the variation of load up to 28 kg. The performances as shown in the results prove that the objective of the proposed controller has been successfully achieved referring to the reduction of the time taken from the stroke to reach the steady state condition.

Conflict of Interests

The authors declare that there is no conflict of interests regarding the publication of this paper.

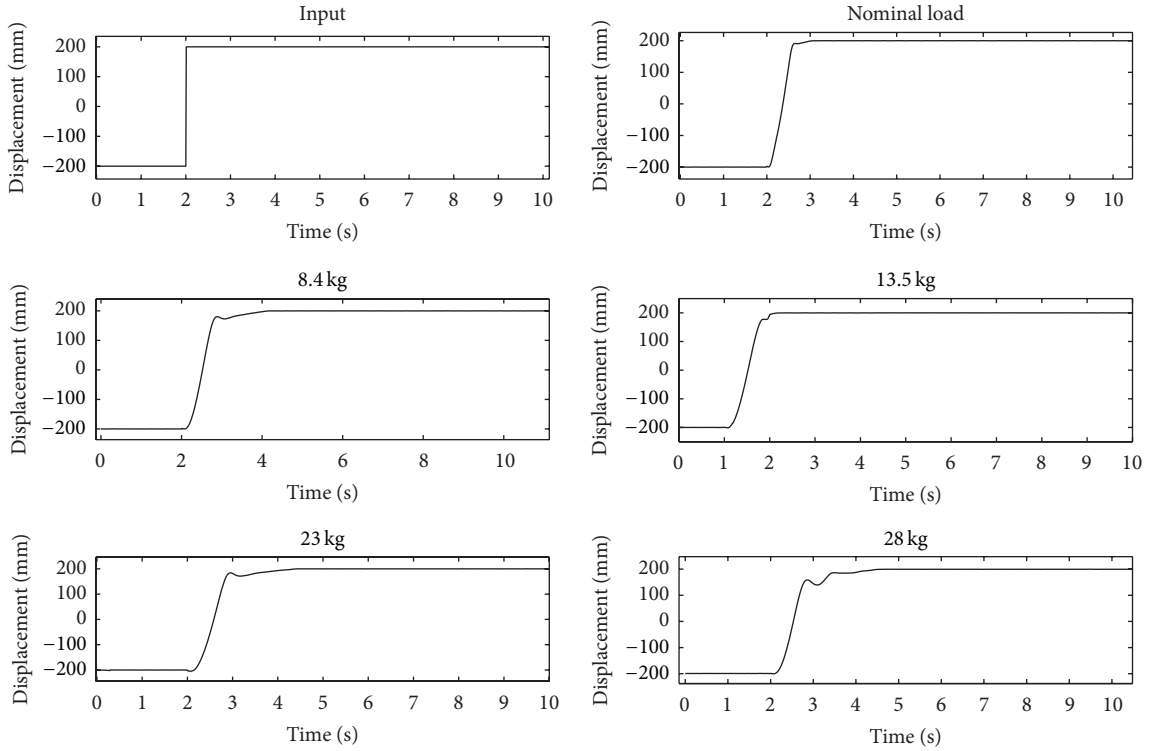

Figure 14: Experimental results under various loads.

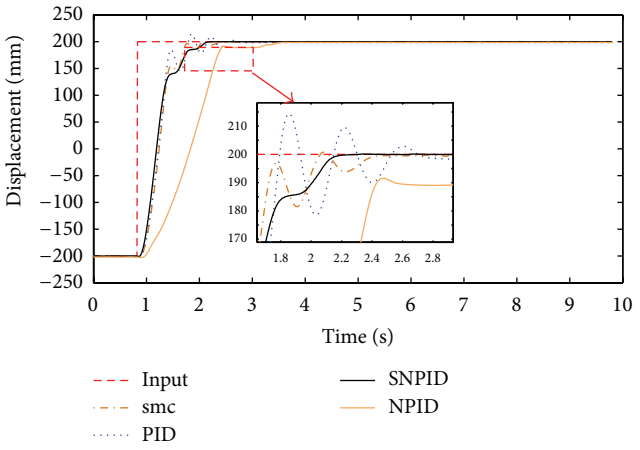

Figure 15: System responses with load 13.5 kg for different controller.

Acknowledgments

This research is supported by Ministry of Higher Education (MOHE) Malaysia, Universiti Teknologi Malaysia (UTM), and Universiti Teknikal Malaysia Melaka (UTeM) through Research University Grant (GUP) Tier 1 vote no. Q.J130000.7123.00H36. Authors are grateful to Ministry, UTM, and UTeM for supporting the present work.

References

[1] A. C. Valdiero, C. S. Ritter, C. F. Rios, and M. Rafikov, "Nonlinear mathematical modeling in pneumatic servo position applications," *Mathematical Problems in Engineering*, vol. 2011, Article ID 472903, 16 pages, 2011.

[2] A. A. M. Faudzi, N. D. M. Mustafa, and K. Osman, "Force control for a pneumatic cylinder using generalized predictive controller approach," *Mathematical Problems in Engineering*, vol. 2014, Article ID 261829, 5 pages, 2014.

[3] T. Shen, K. Tamura, N. Henmi, and T. Nakazawa, "Robust model following controller applied to positioning of pneumatic control valve with friction," in *Proceedings of the IEEE International Conference on Control Applocations*, vol. 1, pp. 512–516, Trieste, Italy, September 1998.

[4] L. Reznik, O. Ghanayem, and A. Bourmistrov, "PID plus fuzzy controller structures as a design base for industrial applications," *Engineering Applications of Artificial Intelligence*, vol. 13, no. 4, pp. 419–430, 2000.

[5] J. Wang, J. Pu, and P. Moore, "A practical control strategy for servo-pneumatic actuator systems," *Control Engineering Practice*, vol. 7, no. 12, pp. 1483–1488, 1999.

[6] E. Richer and Y. Hurmuzlu, "A high performance pneumatic force actuator system: Part 2—nonlinear controller design," *ASME Journal of Dynamic Systems Measurement and Control*, vol. 122, no. 3, pp. 426–434, 2000.

[7] S. R. Pandian, F. Takemura, Y. Hayakawa, and S. Kawamura, "Pressure observer-controller design for pneumatic cylinder actuators," *IEEE/ASME Transactions on Mechatronics*, vol. 7, no. 4, pp. 490–499, 2002.

[8] F. Xiang and J. Wikander, "QFT control design for an approximately linearized pneumatic positioning system," *International Journal of Robust and Nonlinear Control*, vol. 13, no. 7, pp. 675–688, 2003.

[9] H. Schulte and H. Hahn, "Fuzzy state feedback gain scheduling control of servo-pneumatic actuators," *Control Engineering Practice*, vol. 12, no. 5, pp. 639–650, 2004.

[10] K. Ahn and T. Thanh, "Nonlinear PID control to improve the control performance of the pneumatic artificial muscle manipulator using neural network," *Journal of Mechanical Science and Technology*, vol. 19, no. 1, pp. 106–115, 2005.

[11] X. Gao and Z.-J. Feng, "Design study of an adaptive Fuzzy-PD controller for pneumatic servo system," *Control Engineering Practice*, vol. 13, no. 1, pp. 55–65, 2005.

[12] S. Aziz and G. M. Bone, "Automatic tuning of an accurate position controller for pneumatic actuators," in *Proceedings of the IEEE/RSJ International Conference on Intelligent Robots and Systems*, vol. 3, pp. 1782–1788, Victoria, Canada, October 1998.

[13] R. B. van Varseveld and G. M. Bone, "Accurate position control of a pneumatic actuator using on/off solenoid valves," *IEEE/ASME Transactions on Mechatronics*, vol. 2, no. 3, pp. 195–204, 1997.

[14] C. Junyi and C. Binggang, "Fractional-order control of pneumatic position servosystems," *Mathematical Problems in Engineering*, vol. 2011, Article ID 287565, 14 pages, 2011.

[15] Z. Situm, D. Pavkovic, and B. Novakovic, "Servo pneumatic position control using fuzzy PID gain scheduling," *ASME Journal Of Dynamic Systems, Measurement and Control*, vol. 126, no. 2, pp. 376–387, 2004.

[16] S. Cai, S. Wu, and G. Bao, "Cylinder position servo control based on fuzzy PID," *Journal of Applied Mathematics*, vol. 2013, Article ID 375483, 10 pages, 2013.

[17] M. Taghizadeh, F. Najafi, and A. Ghaffari, "Multimodel PD-control of a pneumatic actuator under variable loads," *International Journal of Advanced Manufacturing Technology*, vol. 48, no. 5, pp. 655–662, 2010.

[18] M. F. Rahmat, S. N. S. Salim, N. H. Sunar, A. A. M. Faudzi, Z. H. Ismail, and K. Huda, "Identification and non-linear control strategy for industrial pneumatic actuator," *International Journal of the Physical Sciences*, vol. 7, no. 17, pp. 2565–2579, 2012.

[19] H. Seraji, "A new class of nonlinear PID controllers with robotic applications," *Journal of Robotic Systems*, vol. 15, no. 3, pp. 161–181, 1998.

[20] Y. X. Su, D. Sun, and B. Y. Duan, "Design of an enhanced nonlinear PID controller," *Mechatronics*, vol. 15, no. 8, pp. 1005–1024, 2005.

[21] J. Kennedy and R. Eberhart, "Particle swarm optimization," in *Proceedings of the IEEE International Conference on Neural Networks*, vol. 4, pp. 1942–1948, Perth, Australia, December 1995.

[22] Z.-L. Gaing, "A particle swarm optimization approach for optimum design of PID controller in AVR system," *IEEE Transactions on Energy Conversion*, vol. 19, no. 2, pp. 384–391, 2004.

[23] N. Shu and G. M. Bone, "Experimental comparison of two pneumatic servo position control algorithms," in *Proceedings of the IEEE International Conference on Mechatronics and Automation (ICMA '05)*, vol. 31, pp. 37–42, August 2005.